

# Arabidopsis *PEN2*, a promising gene in upraising penetration resistance against rice necrotrophic fungus *Rhizoctonia solani*

Daraksha Parween<sup>1</sup>, Eram Sultan<sup>1</sup>, Kalpana Dalei<sup>1</sup>, Binod Bihari Sahu<sup>Corresp. 1</sup>

<sup>1</sup> Life Science, National Institute of Technology Rourkela, Rourkela, Odisha, India

Corresponding Author: Binod Bihari Sahu  
Email address: binodbiharisahu@gmail.com

*Rhizoctonia solani*, a soilborne necrotroph, causes sheath blight in rice which poses a major threat to global rice production. Besides rice sheath blight, it has a wide host range of other economically important crops like soybean, sugarcane, maize etc. Despite being the most hostile fungus, the mechanism involved in the *R. solani* pathobiology is poorly understood. Non-host resistance (NHR) is an emerging concept that allows breeders to transfer traits to food crops that would impart a broad-spectrum disease resistance. Several NHR genes are known to function against different pathogens of which Arabidopsis *PEN1*, *PEN2* and *PEN3* have been reported to limit the entry of non-adapted powdery mildews and provide cell wall based defenses against different fungi. Till now, there has been no study regarding the involvement of these *PEN* genes against *R. solani*. In this study, we have screened *pen1*, *pen2-3* and *pen3-1* against *R. solani* to explore their contribution in penetration resistance. Among the three *pen* mutants studied, *pen2-3* allowed maximum penetration during the early hours of infection. *R. solani* colonization was also observed in *pen1* and *pen3-1* but the effect was less drastic than *pen2-3*, suggesting the involvement of *PEN2* in pre-invasive defense. To validate our hypothesis, we screened a complemented *pen2* accession, *PEN2-GFP*, which showed restored penetration resistance comparable to Col-0. Altogether, our results demonstrate that *PEN2* is involved in pre-penetration resistance, and contributes to NHR by enhanced disease resistance to *R. solani*.

1 **Arabidopsis *PEN2*, a promising gene in upraising penetration resistance against rice**  
2 **necrotrophic fungus *Rhizoctonia solani***

3

4 Daraksha Parween, Eram Sultan, Kalpana Dalei and Binod Bihari Sahu\*

5 Laboratory of Molecular Genetics and Plant Immunity, Department of Life Science, National  
6 Institute of Technology Rourkela, Odisha, INDIA, 769008

7

8 \*To whom correspondence may be addressed. E mail: binodbiharisahu@gmail.com

9

10 **Email Addresses:**

11 Daraksha Parween: parweendaraksha8@gmail.com

12 Eram Sultan: sultan.eram@gmail.com

13 Kalpana Dalei: kalpanadalei2034@gmail.com

14 Binod Bihari Sahu: binodbiharisahu@gmail.com

15

16

## 17 Abstract

18 *Rhizoctonia solani*, a soilborne necrotroph, causes sheath blight in rice which poses a major  
19 threat to global rice production. Besides rice sheath blight, it has a wide host range of other  
20 economically important crops like soybean, sugarcane, maize etc. Despite being the most  
21 hostile fungus, the mechanism involved in the *R. solani* pathobiology is poorly understood.  
22 Non-host resistance (NHR) is an emerging concept that allows breeders to transfer traits to  
23 food crops that would impart a broad-spectrum disease resistance. Several NHR genes are  
24 known to function against different pathogens of which Arabidopsis *PEN1*, *PEN2* and  
25 *PEN3* have been reported to limit the entry of non-adapted powdery mildews and provide  
26 cell wall based defenses against different fungi. Till now, there has been no study regarding  
27 the involvement of these *PEN* genes against *R. solani*. In this study, we have screened *pen1*,  
28 *pen2-3* and *pen3-1* against *R. solani* to explore their contribution in penetration resistance.  
29 Among the three *pen* mutants studied, *pen2-3* allowed maximum penetration during the  
30 early hours of infection. *R. solani* colonization was also observed in *pen1* and *pen3-1* but the  
31 effect was less drastic than *pen2-3*, suggesting the involvement of *PEN2* in pre-invasive  
32 defense. To validate our hypothesis, we screened a complemented *pen2* accession, *PEN2*-  
33 *GFP*, which showed restored penetration resistance comparable to Col-0. Altogether, our  
34 results demonstrate that *PEN2* is involved in pre-penetration resistance, and contributes to  
35 NHR by enhanced disease resistance to *R. solani*.

36 **Key Words:** Nonhost resistance; necrotroph; *Rhizoctonia solani*; infection cushion; penetration

## 37 Introduction

38 *Rhizoctonia solani* (teleomorph, *Thanatephorus cucumeris*), a multinucleated filamentous  
39 necrotroph, causes diseases like sheath blight and banded leaf disease in monocots like rice,

40 maize and sorghum; aerial blight and stem rot in legumes like mung bean and soybean; sheath  
41 rot in sugarcane, damping off of cotton, black scurf and sprout canker in potato, heart rot in  
42 cabbage, and foliar blights in other fruits and plantation crops (Ajayi-Oyetunde & Bradley 2018;  
43 Nagaraj et al. 2017). Rice sheath blight is the most devastating disease challenging global food  
44 security amongst other diseases caused by *R. solani* and can potentially cause around 50%  
45 reduction in rice yield worldwide (Zheng et al. 2013). *R. solani* is both soilborne as well as  
46 waterborne pathogen. This non-sporulating fungus survives in the form of sclerotia during the  
47 inactive phases of its infection cycle (KUMAR<sup>1</sup> et al. 2009). Under favorable conditions, these  
48 sclerotias germinate into mycelia which further form atypical hyphal aggregates called infection  
49 cushions, required for host penetration (Kumar et al. 2011; Łazniewska et al. 2012; Singh et al.  
50 2012; Taheri & Tarighi 2011). *R. solani* induces programmed cell death with loss of  
51 photosynthetic activity and development of necrotic lesions in the host tissues (Taheri & Tarighi  
52 2011) (Mondal et al. 2012). It is also reported that the hyphal growth and penetration of *R. solani*  
53 is influenced by protrusions or openings on the leaves of host surface, such as trichomes, stomata  
54 or papillae (Basu et al. 2016).

55 Most of the plant diseases are caused by fungal pathogens (Łazniewska et al. 2012). To fight  
56 against various pathogenic attacks, plant possess immune system with multilayered continuum of  
57 both pre-formed and acquired barriers. The disease resistance is mediated by sequential basal and  
58 resistance (R)-gene mediated hypersensitive response that does not always involve recognition of  
59 pathogenic cues (Gill et al. 2015). Non-host resistance demarcates the host range of  
60 phytopathogenic microorganisms, representing the hallmarks of basic compatibility. Thus,  
61 adapted pathogens always try to suppress or evade the plant's basal defense mechanism by  
62 secreting a repertoire of effector molecules (Speth et al. 2007) against robust and durable nature

63 of NHR as a part of innate immunity (Nuernberger & Lipka 2005). Durability of NHR has  
64 increased attention to revamp resistance in crop. Elaborated suite of plant defense system induces  
65 downstream cell-autonomous responses of PAMP-triggered immunity (PTI) including  
66 production of reactive oxygen species (ROS), MAP-kinase signaling, transcriptional induction of  
67 pathogenesis-related (PR) genes, and callose deposition (Bittel & Robatzek 2007).

68 In Arabidopsis, cell wall based defenses are mediated by three *PENETRATION* genes - *PEN1*,  
69 *PEN2* and *PEN3* and allow limited entry of non-adapted powdery mildews. *PEN1* encodes a  
70 syntaxin (SYP121/PEN1) which belongs to the SNARE superfamily proteins. *PEN1* plays a role  
71 in the papilla formation (Collins et al. 2003). *PEN2* encodes myrosinase, associated with  
72 peroxisomes, which implicates production of glucosinolate derivatives as an antifungal defense  
73 compounds (Bednarek et al. 2009; Lipka et al. 2005). The toxic by-products of *PEN2* are  
74 transported to the sites of pathogen entry by ABC transporter proteins which is encoded by  
75 *PEN3* gene. *PEN2* and *PEN3* have been documented to confer disease resistance against  
76 biotroph *viz. Erysiphe pisi*, hemibiotrophic oomycete *Phytophthora infestans* as well as  
77 necrotroph *P. cucumerina* (Stein et al. 2006).

78 The molecular mechanism of disease resistance to *R. solani* and its mode of infection in hosts are  
79 not clear. Therefore, the objective of this study was to unravel the defense strategies against *R.*  
80 *solani* in non-host wild type Arabidopsis Col-0 and *pen1*, *pen2-3* and *pen3-1* mutants.

81

## 82 Materials and Methods

### 83 Growth and maintenance of Arabidopsis

84 Arabidopsis wild type; Col-0 (N1093), T-DNA insertion line of *pen1* (N673657,  
85 SALK\_004484C), EMS mutants *pen2-3* (N66946) and *pen3-1* (N66467) and complement *PEN2-*  
86 GFP (N67162) were procured from NASC, Europe and were grown in the plant growth chamber.  
87 The plants were grown on soil mixture containing agropeat: vermiculite (3:1), and maintained at  
88 14hour photoperiod with  $\sim 100 \mu\text{E}/\text{m}^2/\text{s}$  light intensity,  $21^\circ\text{C}$  temperature and 60% humidity.

### 89 *Rhizoctonia solani* culture conditions

90 *R. solani* isolate was collected from National Rice Research Institute (NRRI) and was routinely  
91 cultured on freshly prepared potato dextrose agar (PDA) medium supplemented  
92 with antibiotic streptomycin ( $100 \mu\text{g}/\text{mL}$ ). PDA plates were grown for  $\sim 14$  days until  
93 sclerotias developed which were used for infection assay.

### 94 Infection assay

95 Detached leaf assay was performed by taking three upper rosette leaves of 4 week old plants of  
96 Arabidopsis (Mukherjee et al. 2010). Leaves were inoculated with approximately equal sized  
97 ( $\sim 0.3\text{-}0.4$  cm diameter) sclerotia of *R. solani* and maintained in petriplates with 100% humidity.  
98 Infected leaves were harvested at different time points for microscopic and macroscopic  
99 observations. The experiment was carried out three times, and each contained three biological  
100 replicates.

### 101 Microscopy

102 Trypan blue, DAB (3,3'-diaminobenzidine) and aniline blue staining were performed to study  
103 cell death,  $\text{H}_2\text{O}_2$  accumulation and callose deposition respectively, as described by Park et al  
104 (2009) (Park et al. 2009). For trypan blue staining, infected leaves were cleared in alcoholic  
105 lactophenol (2:1) and stained with  $250 \mu\text{g}/\text{mL}$  trypan blue in lactophenol (phenol: glycerol: lactic

106 acid: water – 1:1:1:1, v/v). It was further destained with lactophenol, mounted onto glass slide  
 107 with 50% glycerol and examined under bright field microscope. For DAB staining, infected  
 108 leaves were incubated in 1mg/mL aqueous DAB solution for 8h in dark following which stain  
 109 was replaced with water and incubated in similar conditions. Destaining was performed with  
 110 acetic acid: ethanol (96:4 v/v) and mounted with 50% glycerol and visualized under brightfield  
 111 microscope. For aniline blue staining, leaves were cleared in alcoholic lactophenol and stained  
 112 overnight with 0.01% aniline blue in 150mM K<sub>2</sub>HPO<sub>4</sub>, pH 9.5. stained leaves were equilibrated  
 113 with 50% glycerol and observed under UV excitation.

#### 114 Extraction and Estimation of Chlorophyll content

115 One gram of treated and untreated leaves were taken at 30 and 48hpi and ground with 20 mL of  
 116 80% acetone. It was then centrifuged at 5000 rpm for 5 minutes. The supernatant was collected  
 117 in a tube and the process was repeated until the residue appears colorless. Supernatant was made  
 118 upto 100 mL with 80% acetone. The absorbance of the solution was recorded at 645 nm and 663  
 119 nm against the blank solvent (acetone) (Rajalakshmi & Banu 2013). The concentrations of  
 120 chlorophyll a, chlorophyll b and total chlorophyll was measured as mg/g of the sample and were  
 121 calculated as described by Rafii et al. 2015 (Azizi et al. 2015) using the following equation:

122

$$123 \text{ Chlorophyll a (mg/g Fresh leaf)} = 12.7 \times (A663) - 2.69 \left( \frac{A645}{1000} \right) \times \frac{V}{W}$$

124

$$125 \text{ Chlorophyll b (mg/g Fresh leaf)} = 22.9 \times (A645) - 4.68 \left( \frac{A663}{1000} \right) \times \frac{V}{W}$$

126

$$127 \text{ Total Chlorophyll (mg/g Fresh leaf)} = 20.2 \times (A645) + 8.02 \left( \frac{A663}{1000} \right) \times \frac{V}{W}$$

## 128 Scanning electron microscopy

129 Infected leaves were fixed in 4% paraformaldehyde and subsequently washed with phosphate  
130 buffer. Leaves were blotted dry with kimwipe and mounted on metal stubs for visualization  
131 under environmental SEM. Each plant had a number of three detached leaves and data from three  
132 biological replicates.

## 133 Pathogenicity Assays and calculation of disease level using detached leaves

134 The infected rosette leaves from the wild type and *pen* mutants, harvested at 1dpi, 2dpi and 3dpi  
135 were photographed. The percentage of disease level was calculated based on the area of necrotic  
136 lesions formed at different time point in all accessions of Arabidopsis. At 1dpi, 2dpi and 3dpi,  
137 disease level was calculated in whole plant as follows:

138

$$139 \text{ Percentage of disease level (\%)} = \left( \frac{\text{Area of lesion formed in leaves of a plant}}{\text{total area of leaves of a plant}} \right) \times 100$$

140

141 Each plant had a number of three detached leaves and data from three biological replicates were  
142 taken for calculation. The data were expressed as means  $\pm$  standard error of the mean (SEM).

143

## 144 Results

### 145 *PEN2* is involved in pre-penetration resistance to *R. solani*

146 In order to assess the resistance phenotypes in Arabidopsis wild type Col-0 and penetration  
147 deficient mutants, a T-DNA insertion mutant *pen1* and EMS generated *pen2-3* and *pen3-1* were  
148 used. The *pen* mutants obtained from NASC were confirmed for their homozygosity by using  
149 PCR based analysis (Fig. S1, Supplementary Table 1). Leaves of four weeks old plants were  
150 challenged with *R. solani* sclerotia for 6, 12, 24, 30, 36 and 48 hours post inoculation (hpi). We



151 observed no mycelial growth after 6 and 12hpi in either Col-0 or the *pen* mutants. However, at  
152 24hpi and 30hpi, onset of branching of secondary hyphae were observed in Col-0 but no such  
153 extensive mycelial colonization was observed (Fig. S2). On the other hand, *pen* mutants showed  
154 profuse branching of the fungal hyphae. Among the *pen* mutants, *pen2-3* showed maximum  
155 fungal colonization and initiation of typical infection cushions was observed at 30hpi, which  
156 lacked in wild type as well as *pen1* and *pen3-1*. Prominent infection cushions were clearly visible  
157 at 36hpi and 48hpi in *pen2-3*, which was initiated in *pen3-1* at 48hpi and totally absent in Col-0  
158 and *pen1* (Fig. S2). To further examine the results obtained in previous time course experiment,  
159 we focused our observations on 30hpi where initiation of typical infection cushion was seen in  
160 *pen2-3* and 48hpi where well-formed infection cushions were observed (Fig. 1). Leaves of *pen2-*  
161 *3* showed several runner hyphae entangled together to form lobate appressoria and initiation of  
162 infection cushion at 30hpi. At 48hpi, there was more hyphal proliferation in *pen2-3* which  
163 resulted in formation of compact bundles of fungal hyphae entrenched onto the leaves surface  
164 and the formation of infection cushions (Fig. 1).

#### 165 *R. solani* infection reduces photosynthetic efficiency in *pen2-3*

166 Pathogen virulence leads to the inhibition of photosynthesis (Okorski et al. 2008). Thus, the  
167 disappearance of chlorophyll was analyzed at 30 and 48hpi. Compared to the untreated leaves of  
168 Arabidopsis, treated leaves showed reduced chlorophyll content. Higher amount of chlorophyll  
169 content was recorded in treated leaves of Col-0 with that of *pen* mutants. *pen2-3* showed  
170 maximum degradation in cellular chlorophyll content as compared to wild type, *pen1* and *pen3-1*  
171 which correlate with the microscopic observations (Fig. S3).

172 *pen2-3* triggers the formation of infection cushions

173 We investigated the stages of formation of typical infection cushion of *R. solani* on leaves by  
174 comparing wild type and *pen* mutants by observing under SEM. Col-0 showed secondary hyphal  
175 branching at 30hpi and no infection cushions *pen1* showed almost similar hyphal structure as that  
176 of Col-0 (Fig. S4). However, *pen2-3* at 30hpi, showed profuse mycelial branching and initiation  
177 of infection cushions (Fig. S4) which however was observed in *pen3-1* at 48hpi. At 48hpi, *pen2-*  
178 *3* formed infection cushions which leads the hyphae to a bulbous end forming lobate appressoria  
179 (1a). Aggregation of compact hyphal branches leads to the formation of infection pegs at the base  
180 of the cushion which allows the pathogen to penetrate and proliferate further (Dodman et al.  
181 1968). The growth of the hyphae on the leaf surface of Arabidopsis showed usual right-angled  
182 branching patten of *R. solani*. The infection cushions were found to be present exclusively in  
183 *pen2-3*.

184 *pen* mutants accumulate more H<sub>2</sub>O<sub>2</sub> and callose in response to *R. solani* infection

185 Production of ROS and deposition of callose by plants acts as a major defense response against  
186 biotic stress at the site of plant-pathogen interaction (Fauth et al. 1998; Luna et al. 2011).  
187 Deposition of H<sub>2</sub>O<sub>2</sub> was detected as dark yellowish-brown precipitate (Fig. 2). As expected,  
188 *pen2-3* exhibited relatively higher level of accumulation of H<sub>2</sub>O<sub>2</sub> at more sites of infection,  
189 followed by *pen1* and *pen3-1* as compared to Col-which can be correlated with increased cell  
190 death rate (Fig. 2). Callose deposition was examined using aniline blue stain. The leaves of wild  
191 type showed reduced callose deposition and mutant plants accumulated significantly more  
192 localized callose (Fig. 3). Significantly higher amount of callose deposition was found in the  
193 leaves of infected *pen2-3* among all indicating compromised disease resistance in *pen2-3*,  
194 substantiating the microscopic data.

195 Macroscopic lesion phenotypes induced by *R. solani* vary between wild type and *pen*  
196 mutants of *Arabidopsis*

197 Wild type Col-0 and the *pen* mutants were almost indistinguishable up to 1dpi (days of post  
198 inoculation) with sclerotia of *R. solani*. The wild type became chlorotic upon increasing the  
199 inoculation time up to 3dpi and did not develop much lesions spontaneously. In contrast to that  
200 *pen1*, *pen2-3* and *pen3-1* started showing necrotic lesions along with chlorosis at 2dpi. *pen2-3*  
201 showed maximum necrotic lesion and chlorosis at 2dpi and 3dpi. Macroscopic lesions were  
202 almost identical up to 1dpi. By contrast, when the infection period was increased up to 3dpi,  
203 mutants were clearly distinguished from the wild type, especially as seen in leaves of *pen2-3*  
204 mutant (Fig. 4). Based on this experiment, percentage of disease severity was calculated (Fig.  
205 S5). Wild type Col-0 had an average of 0.09%, 0.55%, 22.08% necrotic tissues at 1dpi, 2dpi and  
206 3dpi respectively (average  $\pm$  standard deviation, n= 5). *pen1* showed an average necrotic lesion  
207 of about 0.102%, 0.064%, 27.06% at 1dpi, 2dpi and 3dpi respectively. On the other hand, *pen2-3*  
208 mutant leaves showed maximum necrotic lesion with an average of 0.139%, 36.38% and 67.54%  
209 at 1dpi, 2dpi and 3dpi respectively. Leaves of *pen3-1* showed relatively lesser necrotic lesions  
210 than *pen2-3* but more than *pen1* and Col-0 with an average of 0.108%, 2.71% and 43.54% at  
211 1dpi, 2dpi and 3dpi respectively.

212 *PEN2* provides penetration resistance against *R. solani*

213 To authenticate the result that *pen2-3* mutant triggers cushion formation, we targeted  
214 complement line expressing green fluorescent protein (GFP)-*PEN2*, driven by native 5'  
215 regulatory region in *PEN2-1* background. Due to the knockdown of *PEN2*, *pen2-3* allowed the  
216 formation of infection cushions on the leaves surface. Furthermore, the complemented line  
217 (*PEN2*-GFP) for the *pen2-3* mutant, behaved similar to wild type Col-0 with no cushion

218 formation at 30hpi and 40hpi in response to *R. solani* (Fig. 5). This experiment corroborated our  
219 hypothesis that *PEN2* enhance penetration resistance against *R. solani*.

## 220 Discussion

221 For a successful plant- pathogen interaction, the pathogen recognizes a surface for the initiation  
222 of its growth and further penetrates into the host tissue to cause infection. Non-host resistance  
223 provides durable protection against invading pathogens by using various defense strategies  
224 (Thordal-Christensen 2003). The coherent investigation of our present study revealed that *pen2-3*  
225 contributes to non-host resistance in *Arabidopsis thaliana* to *Rhizoctonia solani*, a necrotrophic  
226 rice pathogen. Among the *pen* mutants, including *pen1*, *pen2-3* and *pen3-1*, *pen2-3* was observed  
227 with compromised penetration resistance to *R. solani*. *pen2-3* showed maximum number of  
228 atypical infection cushions which clearly depicts the important role playing in non-host  
229 resistance against sheath blight in rice.

230 Flentje (1963) reported that the infection cushions develops only in the susceptible host which is  
231 suppressed in the resistant host (Flentje et al. 1963). Despite having very less in-depth studies  
232 about the mechanism of infection process of *R. solani* in various host, it is reported that *R. solani*  
233 produces typical infection structure by forming cluster of hyphae with bulbous end during its  
234 pre-penetration stage(Łażniewska et al. 2012). This clustering T-shaped branched hyphae and  
235 formation of infection cushions further leads to penetration by defeating the barriers present in  
236 the host tissue, enters via penetration peg and promotes colonization (Pannecoucq & Höfte  
237 2009). To fight against the invasion of pathogens, Arabidopsis have penetration genes (*PEN*)  
238 which avoid penetration and is responsible for fast defense response against various non host  
239 fungal pathogens.

240 The primary objective of our study was to evaluate the role of *PEN* genes of Arabidopsis in  
241 providing resistance against *R. solani*. Till now, no non-host resistance (NHR) gene has been  
242 reported that provides disease resistance against the necrotrophic fungus- *Rhizoctonia solani*  
243 with broad range host. We screened the Arabidopsis *PEN* genes, including *PEN1*, *PEN2* and  
244 *PEN3*, among which it was found that *PEN2-3* provides disease resistance against rice sheath  
245 blight pathogen *R. solani* for the first time. As per the previous report by Lazniewska et al.  
246 (2012), we observed the formation of similar infection cushions in *pen2-3* mutants upon  
247 infection with *R. solani*. Unlike *pen2-3*, *pen1* and *pen3-1* mutants did not allow the formation of  
248 infection cushion at 30hpi (Fig. 1). In *pen3-1*, the runner hyphae gave rise to swollen hyphal tips  
249 instead of forming cushion like structures. This experiment made it quite apparent that there is a  
250 clear distinction between hyphal branching formed by wild type and infection cushion formed by  
251 *pen2-3*.

252 To dissect the role of *PEN* genes of Arabidopsis in conferring non-host resistance against *R.*  
253 *solani* further, we performed DAB and Aniline blue staining. The observation from DAB  
254 staining clearly indicated the production of H<sub>2</sub>O<sub>2</sub> in *pen2-3* at many places where there is site of  
255 interaction from cushions of the mycelia and Arabidopsis epidermal cells as compared with  
256 *pen1*, *pen3-1* and wild type Col-0. As it is already reported that the production of H<sub>2</sub>O<sub>2</sub> not only  
257 provide direct defense response but also follows signal transduction pathway which lead to  
258 hypersensitive response (HR) (Waetzig et al. 1999). The production of H<sub>2</sub>O<sub>2</sub> was not only  
259 observed at the site of infection in *pen2-3* but also in the neighboring cells of the inoculated  
260 leaves which signifies that neighboring cells defense system has already activated and shows up  
261 HR response by following signaling. Contrastingly, *pen1* showed reduced peroxidase activity at  
262 the early hour of infection. *pen3-1* showed little higher accumulation of H<sub>2</sub>O<sub>2</sub> than *pen1* but less

263 than *pen2-3* (Fig. 2). Thus, higher production of H<sub>2</sub>O<sub>2</sub> in *pen2-3* at an early stage may indicate  
264 the pathway activating the early signaling event are intact in the mutant.

265 Production of callose; composed of  $\beta$ -(1,3)-glucan polymer, serves as a biomarker against  
266 intrusion by pathogens at the site of infection in host (Luna et al. 2011). Callose deposition  
267 varied in all the three *pen* mutants. *pen1* failed to produce enhanced callose in response to *R.*  
268 *solani* infection. In contrast to *pen2-3* which showed thick callose deposition at the site of  
269 infection, *pen1* showed patch like pattern (Fig. 3). The notable increase in the deposition of  
270 callose in *pen2-3* mutant may explain the number and extent of attempted sites of fungal  
271 penetration. Previously it is reported that papillae composed of callose are deposited at the sites  
272 of penetration into the cell wall by the fungal pathogen, which results in the cell wall thickening  
273 (Ellinger et al. 2013).

274 Macroscopic infection symptom results clearly showed the elevation in lesion formation. This  
275 results correlates with the increased formation of infection cushions in *pen2-3* (Fig. 4). Further,  
276 chlorosis, declination in chlorophyll level, higher necrotic lesions and increased leaf senescence  
277 in *pen2-3* mutant leaves suggested that *pen2-3* was most susceptible among the other two *pen*  
278 mutants. Confirmation from the infection of complement line of *pen2-3* showed similar behavior  
279 as that of Col-0 (Fig. 5).

280 In summary, our study has uncovered the involvement of *PEN2* gene from Arabidopsis at pre-  
281 penetration stage which is an early infection process in providing disease resistance against  
282 broad host range pathogen *R. solani* which has not been reported previously. Further,  
283 characterization of the genes in multiple plant hormone pathway mutants might show clear idea  
284 on the involvement of the genes in NHR disease resistance against rice sheath blight.

285

286 

## Acknowledgement

287 We thank Director NIT Rourkela for providing all facilities and Sushant Pradhan for his  
288 technical assistance in Confocal facility at NIT Rourkela, Odisha INDIA. This work was  
289 supported by the grants from S & T division, Govt. of Odisha (Grant number 27552800232014)  
290 and SERB, Govt. of India (YSS/2014/000142) to the principal investigator. We thank Dr. Arup  
291 K. Mukherjee, NRRI, Cuttack for providing the *R. solani* pure culture.

292

293 

## References

- 294 Ajayi-Oyetunde O, and Bradley C. 2018. *Rhizoctonia solani*: taxonomy, population biology and  
295 management of rhizoctonia seedling disease of soybean. *Plant pathology* 67:3-17.
- 296 Azizi P, Rafii MY, Mahmood M, Abdullah SN, Hanafi MM, Nejat N, Latif MA, and Sahebi M. 2015.  
297 Differential gene expression reflects morphological characteristics and physiological processes in  
298 rice immunity against blast pathogen *Magnaporthe oryzae*. *PloS one* 10:e0126188.
- 299 Basu A, Chowdhury S, Ray Chaudhuri T, and Kundu S. 2016. Differential behaviour of sheath blight  
300 pathogen *Rhizoctonia solani* in tolerant and susceptible rice varieties before and during  
301 infection. *Plant pathology* 65:1333-1346.
- 302 Bednarek P, Piślewska-Bednarek M, Svatoš A, Schneider B, Doubský J, Mansurova M, Humphry M,  
303 Consonni C, Panstruga R, and Sanchez-Vallet A. 2009. A glucosinolate metabolism pathway in  
304 living plant cells mediates broad-spectrum antifungal defense. *science* 323:101-106.
- 305 Bittel P, and Robatzek S. 2007. Microbe-associated molecular patterns (MAMPs) probe plant immunity.  
306 *Current opinion in plant biology* 10:335-341.
- 307 Collins NC, Thordal-Christensen H, Lipka V, Bau S, Kombrink E, Qiu J-L, Hüchelhoven R, Stein M,  
308 Freialdenhoven A, and Somerville SC. 2003. SNARE-protein-mediated disease resistance at the  
309 plant cell wall. *Nature* 425:973.
- 310 Dodman R, Barker K, and Walker J. 1968. A detailed study of the different modes of penetration by  
311 *Rhizoctonia solani*. *Phytopathology* 58:1271-1276.
- 312 Ellinger D, Naumann M, Falter C, Zwikowics C, Jamrow T, Manisseri C, Somerville SC, and Voigt CA. 2013.  
313 Elevated early callose deposition results in complete penetration resistance to powdery mildew  
314 in *Arabidopsis*. *Plant physiology*:pp. 112.211011.
- 315 Fauth M, Schweizer P, Buchala A, Markstädter C, Riederer M, Kato T, and Kauss H. 1998. Cutin  
316 monomers and surface wax constituents elicit H<sub>2</sub>O<sub>2</sub> in conditioned cucumber hypocotyl  
317 segments and enhance the activity of other H<sub>2</sub>O<sub>2</sub>elicitors. *Plant physiology* 117:1373-1380.
- 318 Flentje N, Dodman R, and Kerr A. 1963. The mechanism of host penetration by *Thanatephorus*  
319 *cucumeris*. *Australian Journal of Biological Sciences* 16:784-799.

- 320 Gill US, Lee S, and Mysore KS. 2015. Host versus nonhost resistance: distinct wars with similar arsenals.  
321 *Phytopathology* 105:580-587.
- 322 KUMAR<sup>1</sup> KVK, REDDY<sup>1</sup> M, KLOEPPER<sup>1</sup> J, LAWRENCE<sup>1</sup> K, Groth D, and Miller M. 2009. Sheath blight disease  
323 of rice (*Oryza sativa* L.)-An overview.
- 324 Kumar KVK, Reddy M, Yellareddygar S, Kloepper J, Lawrence K, Zhou X, Sudini H, and Miller M. 2011.  
325 Evaluation and selection of elite plant growth-promoting rhizobacteria for suppression of sheath  
326 blight of rice caused by *Rhizoctonia solani* in a detached leaf bio-assay. *International Journal of*  
327 *Applied Biology and Pharmaceutical Technology* 2:488-495.
- 328 Łażniewska J, Macioszek VK, and Kononowicz AK. 2012. Plant-fungus interface: the role of surface  
329 structures in plant resistance and susceptibility to pathogenic fungi. *Physiological and Molecular*  
330 *Plant Pathology* 78:24-30.
- 331 Lipka V, Dittgen J, Bednarek P, Bhat R, Wiermer M, Stein M, Landtag J, Brandt W, Rosahl S, and Scheel D.  
332 2005. Pre-and postinvasion defenses both contribute to nonhost resistance in *Arabidopsis*.  
333 *science* 310:1180-1183.
- 334 Luna E, Pastor V, Robert J, Flors V, Mauch-Mani B, and Ton J. 2011. Callose deposition: a multifaceted  
335 plant defense response. *Molecular Plant-Microbe Interactions* 24:183-193.
- 336 Mondal A, Dutta S, Nandi S, Das S, and Chaudhuri S. 2012. Changes in defence-related enzymes in rice  
337 responding to challenges by *Rhizoctonia solani*. *Archives of phytopathology and plant protection*  
338 45:1840-1851.
- 339 Mukherjee AK, Carp M-J, Zuchman R, Ziv T, Horwitz BA, and Gepstein S. 2010. Proteomics of the  
340 response of *Arabidopsis thaliana* to infection with *Alternaria brassicicola*. *Journal of proteomics*  
341 73:709-720.
- 342 Nagaraj B, Sunkad G, Pramesh D, Naik M, and Patil M. 2017. Host range studies of rice sheath blight  
343 fungus *Rhizoctonia solani* (Kuhn). *Int J Curr Microbiol App Sci* 6:3856-3864.
- 344 Nuernberger T, and Lipka V. 2005. Non-host resistance in plants: new insights into an old phenomenon.  
345 *Molecular plant pathology* 6:335-345.
- 346 Okorski A, Olszewski J, Pszczółkowska A, and Kulik T. 2008. Effect of fungal infection and the application  
347 of the biological agent EM 1TM on the rate of photosynthesis and transpiration in pea (*Pisum*  
348 *sativum* L.) leaves. *Polish Journal of Natural Sciences* 23:35-47.
- 349 Pannecoucq J, and Höfte M. 2009. Interactions between cauliflower and *Rhizoctonia anastomosis*  
350 groups with different levels of aggressiveness. *BMC Plant Biology* 9:95.
- 351 Park J-Y, Jin J, Lee Y-W, Kang S, and Lee Y-H. 2009. Rice blast fungus (*Magnaporthe oryzae*) infects  
352 *Arabidopsis* via a mechanism distinct from that required for the infection of rice. *Plant*  
353 *physiology* 149:474-486.
- 354 Rajalakshmi K, and Banu N. 2013. Extraction and estimation of chlorophyll from medicinal plants.  
355 *International Journal of Science and Research*:209-012.
- 356 Singh A, Rohila R, WILLOCQUET SSL, and SINGH U. 2012. Infection process in sheath blight of rice caused  
357 by *Rhizoctonia solani*. *Indian Phytopathology*.
- 358 Speth EB, Lee YN, and He SY. 2007. Pathogen virulence factors as molecular probes of basic plant cellular  
359 functions. *Current opinion in plant biology* 10:580-586.
- 360 Stein M, Dittgen J, Sánchez-Rodríguez C, Hou B-H, Molina A, Schulze-Lefert P, Lipka V, and Somerville S.  
361 2006. *Arabidopsis* PEN3/PDR8, an ATP binding cassette transporter, contributes to nonhost  
362 resistance to inappropriate pathogens that enter by direct penetration. *The Plant Cell* 18:731-  
363 746.
- 364 Taheri P, and Tarighi S. 2011. Cytomolecular aspects of rice sheath blight caused by *Rhizoctonia solani*.  
365 *European journal of plant pathology* 129:511-528.
- 366 Thordal-Christensen H. 2003. Fresh insights into processes of nonhost resistance. *Current opinion in*  
367 *plant biology* 6:351-357.



368 Waetzig GH, Sobczak M, and Grundler FM. 1999. Localization of hydrogen peroxide during the defence  
369 response of *Arabidopsis thaliana* against the plant-parasitic nematode *Heterodera glycines*.  
370 *Nematology* 1:681-686.

371 Zheng A, Lin R, Zhang D, Qin P, Xu L, Ai P, Ding L, Wang Y, Chen Y, and Liu Y. 2013. The evolution and  
372 pathogenic mechanisms of the rice sheath blight pathogen. *Nature communications* 4:1424.

## 373 Supplementary Figure Legends Information

### 374 **S1. PCR based confirmation of homozygous *PENETRATION* mutants used in the study.** (a)

375 the T-DNA insertion mutant of *pen1* (SALK\_004484C) was confirmed using a T-DNA left

376 border primer indicating the presence of insert in the mutant. (b) *pen2-3* was confirmed using a

377 CAPS marker indicating the presence of an additional restriction site for *BsmAI* restriction

378 enzyme. (c) *pen3-1* was also confirmed using a CAPS marker showing deletion of *HphI*

379 restriction site in the mutant.

### 380 **S2. Infection phenotypes of *Arabidopsis* wild type and *pen* mutants upon infection with *R.***

381 *solani*. Leaves of Col-0 and *pen* mutants were stained with trypan blue after 6, 12, 24, 30, 36 and

382 48hpi to observe the extent of disease progression. Stained leaves were observed under bright

383 field microscope. Leaves inoculated with water were used as control. Scale bar = 100 $\mu$ m

### 384 **S3. Total chlorophyll estimation upon infection with *R. solani* on *Arabidopsis* wild type**

385 **(Col-0) and *pen* mutants.** Total chlorophyll content measured in leaves of wild type and *pen*

386 mutants of *A. thaliana* after 30 and 48hpi with *R. solani* sclerotia. Leaves treated with water

387 served as control. Data represent the mean  $\pm$  SEM of three biological replicates ( $n = 3$ ). The

388 experiment was carried out three times with similar results.

### 389 **S4. SEM micrographs of *Arabidopsis pen* mutants showing post infection hyphal**

390 **colonization by *R. solani* at 30hpi and 48hpi.** Leaves of *Arabidopsis* wild type (Col-0) and *pen*

391 mutants inoculated with water as control. Col-0 and *pen* mutants inoculated with *R. solani*

392 sclerotia showed disease progression with profuse hyphal branching after 30hpi. *pen2-3* showed

393 sporadic onset of infection cushion formation (ioc; dashed arrow) after 30hpi. Col-0 and *pen*  
394 mutants inoculated with *R. solani* sclerotia observed after 48hpi. Dense infection cushions (ic;  
395 solid arrows) at 48hpi in *pen2-3*. Swollen hyphal tip formed lobate appresoria (la) at 48hpi in  
396 *pen3-1*. Scale bar ~ 50µm

397 **S5. Macroscopic quantification of disease severity of *R. solani* infected Arabidopsis *pen***  
398 **mutants.** Macroscopic necrotic lesions were quantified in terms of area using ImageJ software  
399 after 1, 2 and 3dpi. Data represent percentage mean area ± SEM (n=5).

400 **Supplementary Table 1: List of primers used in the study.**

#### 401 Figure Legends

402 Fig.1. **Formation of infection cushion upon infection with *Rhizoctonia solani* on Arabidopsis**  
403 **wild type (Col-0) and *pen* mutants.** Leaves of wild type and *pen* mutants of Arabidopsis were  
404 stained with trypan blue after 30hpi and 48hpi. Maximum cushions formed at 48hpi in *pen2-3*.  
405 Infection cushions are indicated by arrows. The experiment was carried out three times, and each  
406 contained three biological replicates. Scale bar ~ 50µm.

407 Fig.2. **DAB staining.** Leaves of wild type and *pen* mutants of Arabidopsis were stained with  
408 DAB after 30hpi and 48hpi. Production of H<sub>2</sub>O<sub>2</sub> was observed at the site of infection as  
409 yellowish-brown precipitate. Each experiment was carried out with three biological replicates.  
410 Scale bar-50µm.

411 Fig.3. **Accumulation of callose at sites of infection in Arabidopsis leaves.** Leaves of wild type  
412 and *pen* mutants of Arabidopsis were stained with aniline blue after 30hpi and 48hpi. Callose  
413 deposition was observed UV excitation of a fluorescence microscope. Scale bar = 50µm.

414 Fig.4. **Macroscopic quantification of disease progression in Arabidopsis wild type and *pen***  
415 **mutants.** Four week old plants were infected with *R. solani* sclerotia and photographed at 0dpi,  
416 1dpi, 2dpi and 3dpi. Leaves inoculated with water were used as control. The coverage of necrotic  
417 lesions increased with time in each accession with *pen2-3* being the most affected. The  
418 experiment was carried out three times, and each contained three biological replicates.

419 Fig.5. **Comparison of infection structure of *PEN2-GFP* and *pen2-3* as compared to wild**  
420 **type Col-0.** Leaves of wild type Col-0, PEN2-GFP and *pen2-3* mutants of Arabidopsis were  
421 stained with trypan blue after 30hpi and 48hpi. Maximum cushions formed at 48hpi in *pen2-3*.  
422 Infection cushions are indicated by arrows. Scale bar ~ 50µm.

423

# Figure 1

Formation of infection cushion upon infection with *Rhizoctonia solani* on Arabidopsis wild type (Col-0) and *pen* mutants

Leaves of wild type and *pen* mutants of Arabidopsis were stained with trypan blue after 30hpi and 48hpi. Maximum cushions formed at 48hpi in *pen2-3*. Infection cushions are indicated by arrows. The experiment was carried out three times, and each contained three biological replicates. Scale bar ~ 50µm.

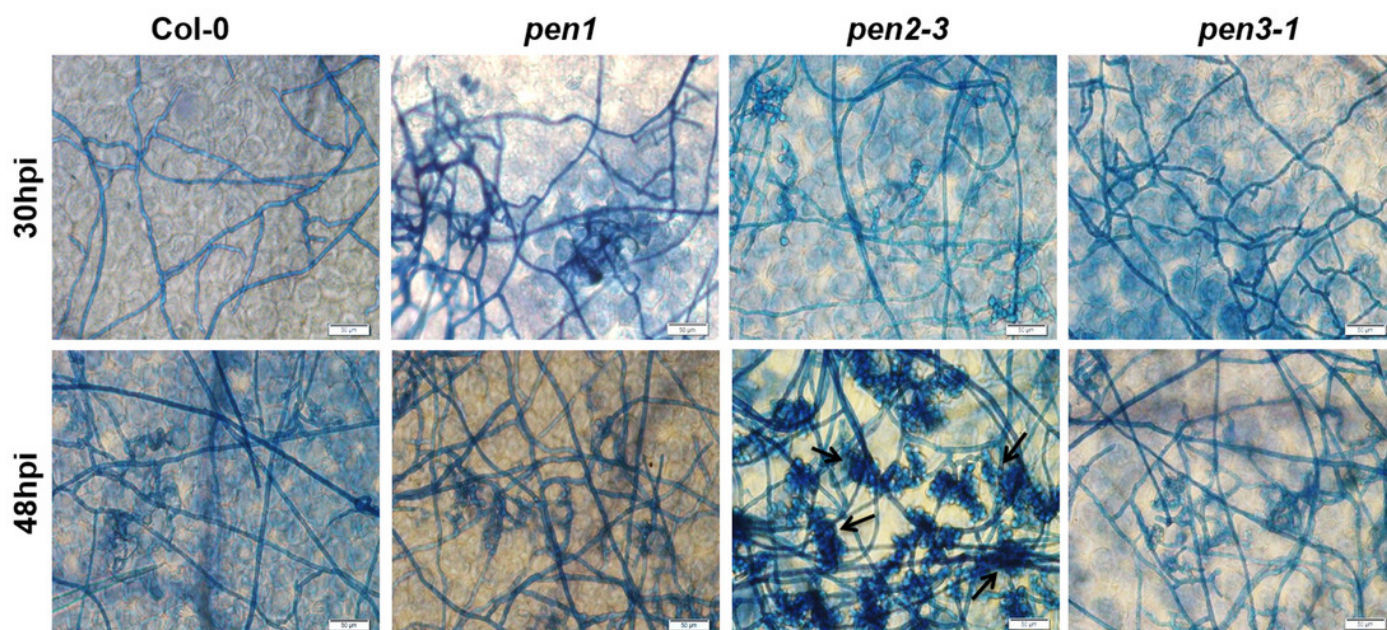


## Figure 2

### DAB staining

Leaves of wild type and pen mutants of Arabidopsis were stained with DAB after 30hpi and 48hpi. Production of  $H_2O_2$  was observed at the site of infection as yellowish-brown precipitate. Each experiment was carried out with three biological replicates. Scale bar-50 $\mu$ m.

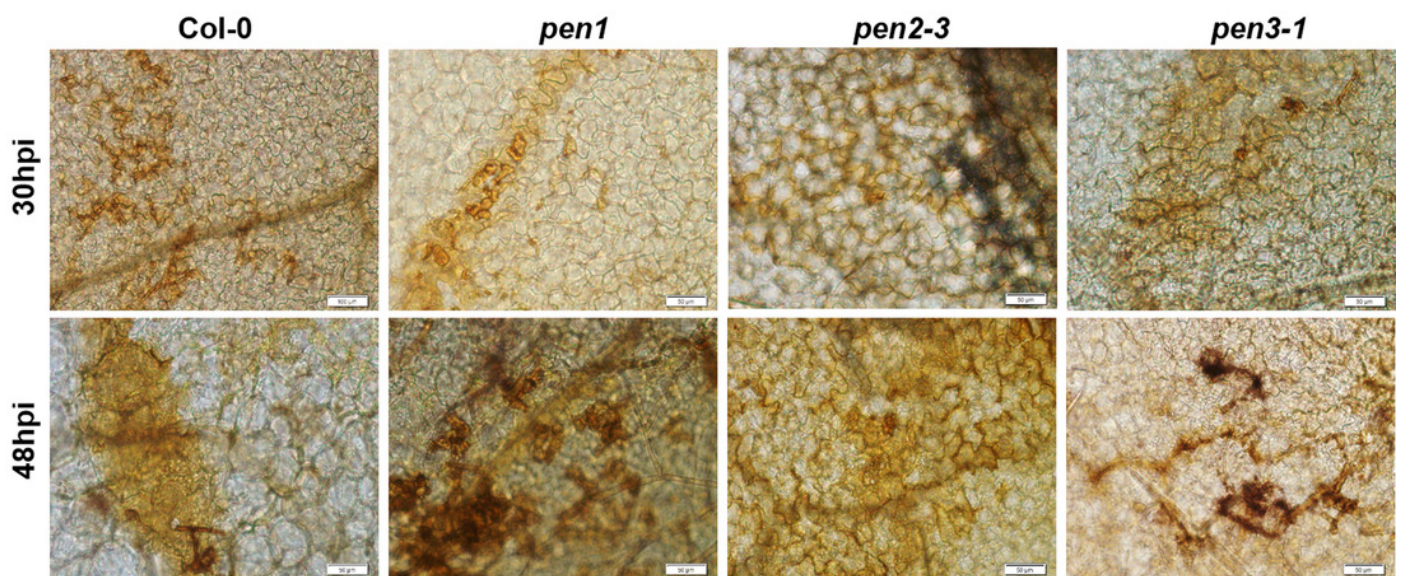


## Figure 3

Accumulation of callose at sites of infection in Arabidopsis leaves

Leaves of wild type and *pen* mutants of Arabidopsis were stained with aniline blue after 30hpi and 48hpi. Callose deposition was observed UV excitation of a fluorescence microscope.

Scale bar = 50 $\mu$ m.

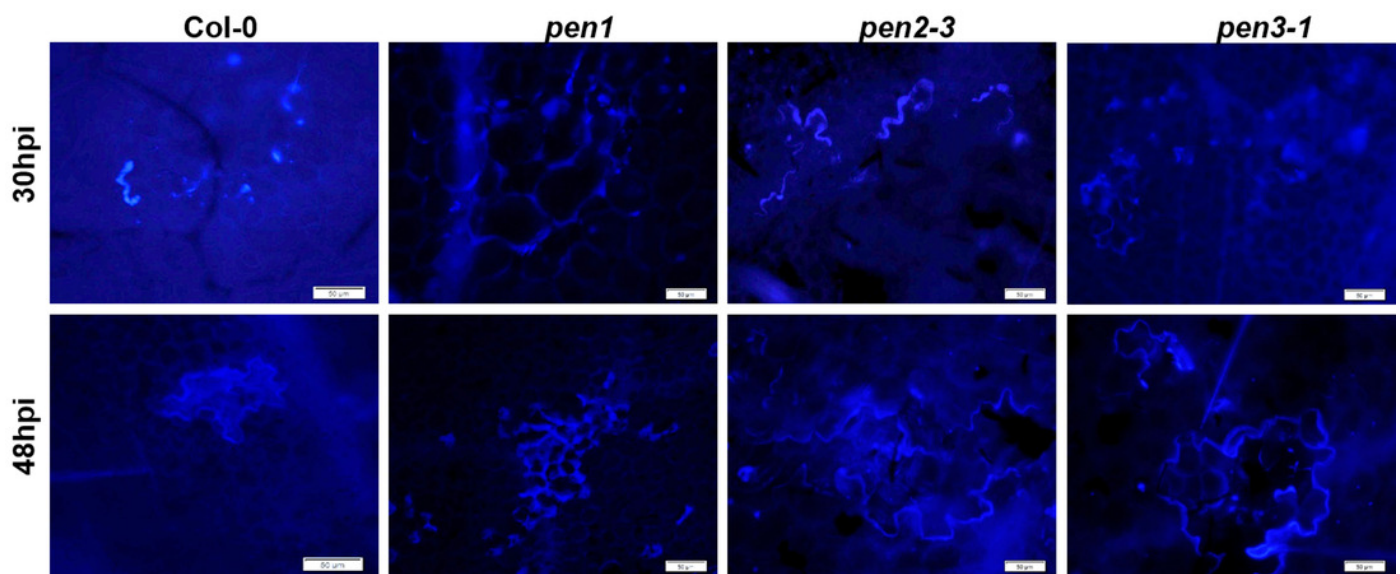


## Figure 4

Macroscopic quantification of disease progression in Arabidopsis wild type and *pen* mutants

Four week old plants were infected with *R. solani* sclerotia and photographed at 0dpi, 1dpi, 2dpi and 3dpi. Leaves inoculated with water were used as control. The coverage of necrotic lesions increased with time in each accession with *pen2-3* being the most affected. The experiment was carried out three times, and each contained three biological replicates.

## Days of post inoculation (dpi)

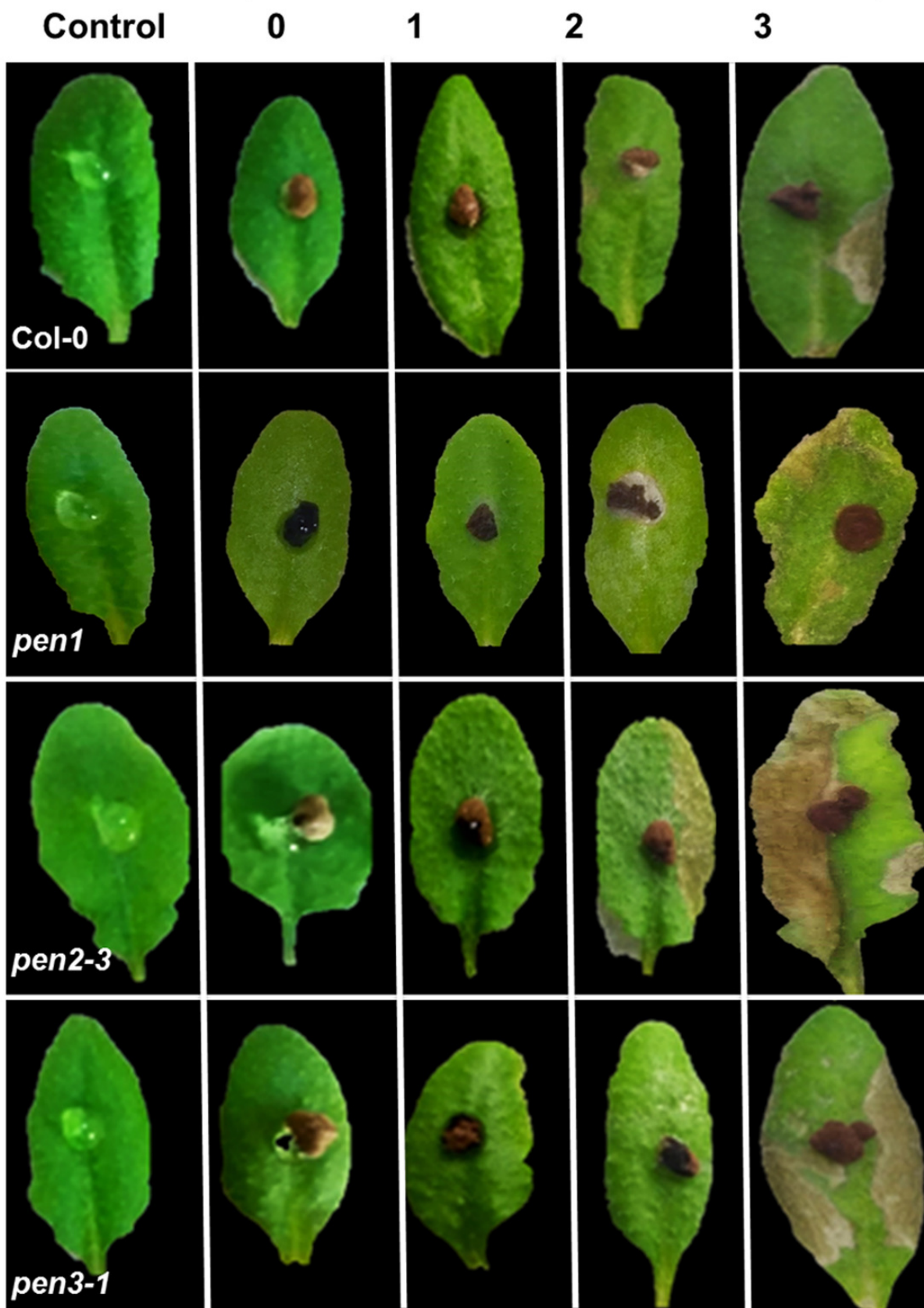




## Figure 5

Comparison of infection structure of *PEN2-GFP* and *pen2-3* as compared to wild type Col-0

Leaves of wild type Col-0, *PEN2-GFP* and *pen2-3* mutants of Arabidopsis were stained with trypan blue after 30hpi and 48hpi. Maximum cushions formed at 48hpi in *pen2-3*. Infection cushions are indicated by arrows. Scale bar ~ 50 $\mu$ m.

